Hydrometallurgy 206 (2021) 105754

Contents lists available at ScienceDirect

Hydrometallurgy

journal homepage: www.elsevier.com/locate/hydromet

A cleaner approach for recovering Al and Ti from coal fly ash via microwave-assisted baking, leaching, and precipitation

Yiqian Ma [a,b,*], Srecko Stopic [a,*], Buhle Xakalashe [a,c], Sehliselo Ndlovu [d], Kerstin Forsberg [b], Bernd Friedrich [a]

[a] Institute of Process Metallurgy and Metal Recycling (IME), RWTH Aachen University, Intzestraße 3, 52056 Aachen, Germany
[b] Department of Chemical Engineering, KTH Royal Institute of Technology, Teknikringen 42, 11428 Stockholm, Sweden
[c] Pyrometallurgy Division, MINTEK, 200 Malibongwe Drive, 2125 Randburg, South Africa
[d] School of Chemical and Metallurgical Engineering, University of the Witwatersrand, P/Bag 3, Wits 2050, 1 Jan Smuts Avenue, Johannesburg, South Africa

ARTICLE INFO

Keywords:
Coal fly ash
Microwave-assisted baking
Leaching
Precipitation
Aluminum
Titanium

ABSTRACT

Coal fly ash (CFA) is a potential mineral resource from which to recover Al and other valuable metals. In this study, a new processing technology for the recovery of Al and Ti from CFA has been developed and comprehensively investigated. The baking process applied in previous work has been improved by using microwave heating and a mixture of H_2SO_4 + NH_4HSO_4 as the extractant. This method enhanced the Al and Ti extraction efficiencies, while decreasing energy consumption and gas emissions relative to other acidic baking processes. When employing the optimized baking and leaching parameters (baking conditions: 280 °C, 1.2 times the theoretical amount of reagents, 60 min; leaching conditions: 60 °C, L/S: 5 g water to 1 g baked ash, 30 min) 82.4% Al and 55.6% Ti could be extracted. Scanning electron microscopy images and X-ray diffraction analysis indicated that most of the mullite ($3Al_2O_3.2SiO_2$) in the CFA was transformed into godovikovite ($NH_4Al(SO_4)_2$) and quartz (SiO_2) after microwave-assisted baking. The soluble salts were then leached into solution, while the quartz remained in the residue. Precipitation allowed for the recovery and separation of Al and Ti from the leach solution. Al was selectively recovered via $NH_4Al(SO_4)_2{\cdot}12H_2O$ precipitation after maintaining the solution at 0 °C for 10 h. A high-quality product of alumina was obtained from the $NH_4Al(SO_4)_2{\cdot}12H_2O$. After reducing the iron in the solution from Fe^{3+} to Fe^{2+}, Ti was recovered via hydrolysis after increasing the pH to 3.1. The Ti precipitate contained 44.2% Ti with a small amount of impurity. The developed approach was cleaner and more efficient than those reported to date for the recovery of Al and Ti from stable CFA.

1. Introduction

Coal fly ash (CFA) consists of fine particles output from a coal-fired furnace at a power station (Lekgoba, Ntuli, and Falayi, 2020). Large amounts of CFA are produced by coal-fired power stations every year, especially in countries where fossil fuel-derived energy is prevalent (Guo et al., 2017; Matjie et al., 2005; Yadav and Fulekar, 2020; Yao et al., 2014). Eskom is the largest supplier of electricity in South Africa, and it produced 34.4 million tons of ash while generating electricity in 2015 (Eskom, 2017). Very little of this CFA is currently recycled for use as building materials, construction fillers, and road bases (Cavusoglu et al., 2020; Shemi et al., 2012; Wei et al., 2018; Yao et al., 2015). Consequently, CFA disposal is becoming a significant concern because it poses a critical threat to the environment (Gupta et al., 2020; Shi, 2020). The extraction of valuable metals from CFA using hydrometallurgical treatments has garnered recent attention because CFA also represents a potential mineral resource (Rampou et al., 2017; Sahoo et al., 2016; Yakaboylu et al., 2019). Importantly, CFA contains a large quantity of aluminum and silica compounds, and small concentrations of critical metals such as Ti and rare earth elements (European Commission, 2020; Matjie et al., 2005; Sahoo et al., 2016; Taggart et al., 2018).

The alumina content in CFA always exceeds 30%, so methods for Al extraction from CFA have been studied extensively (Ding et al., 2017; Li et al., 2014; Shemi et al., 2012; Xue et al., 2019; Yao et al., 2014). Another valuable metal present in relatively high content (>1%) in CFA is Ti, which could easily follow Al during the treatment (Matjie et al., 2005; Rampou et al., 2017). Extraction of other metals depends on their content levels in CFA (Ding et al., 2017; Shemi et al., 2012; Shemi et al.,

* Corresponding authors at: Institute of Process Metallurgy and Metal Recycling (IME), RWTH Aachen University, Intzestraße 3, 52056 Aachen, Germany.
E-mail addresses: yiqianm@kth.se (Y. Ma), sstopic@ime-aachen.de (S. Stopic).

https://doi.org/10.1016/j.hydromet.2021.105754
Received 14 April 2021; Received in revised form 12 September 2021; Accepted 16 September 2021
Available online 28 September 2021
0304-386X/

2015; Taggart et al., 2018). In general, such metal extractions depend highly on the decomposition of aluminosilicates, which are the main phases in CFA and commonly contain embedded phases of other metals. Direct acid leaching at ambient temperature and pressure is not a viable method for decomposing CFA to extract metals because aluminosilicates tend to be very stable under such conditions (Taggart et al., 2018). Therefore, before leaching, the CFA is typically first digested using acid or alkali media at high temperatures and activated with additives to complete the decomposition. Alkali-assisted digestion involves the use of CaO, NaOH, or Na_2CO_3 sintering at high temperature (>700 °C) (Guo et al., 2017; Padilla and Sohn, 1985; Rahaman et al., 2013). Recently, Wei et al. (Wei et al., 2018) studied the acid digestion of Chinese CFA at 300 °C with 98% H_2SO_4 and found that the aluminum extraction efficiency was greater than 80%, but acidic fumes (SO_3) were produced despite the relatively lower temperature. Researchers from South Africa studied the decomposition of CFA using ammonium salts (e.g., NH_4HSO_4 and $(NH_4)_2SO_4$) and baking the CFA at 400–500 °C to extract Al (Doucet et al., 2016; van der Merwe et al., 2017). However, it was determined that the Al extraction efficiency was still lower than 50%, only about 20% of the Ti was extracted, and the mullite ($3Al_2O_3{\cdot}2SiO_2$) component of CFA was barely decomposed. Moreover, NH_3 emission was ignored in this method, and excess extractant was required because NH_4HSO_4 and $(NH_4)_2SO_4$ decomposed at 400–500 °C to produce NH_3 (Zhou et al., 2017). To achieve cleaner production, it is crucial to reduce energy consumption and control the emission of harmful gases.

The principle of microwave heating is converting electromagnetic energy into thermal energy within materials that can absorb microwave energy (Mishra and Sharma, 2016). Microwave radiation has been employed widely in extractive metallurgy because it allows for selective, rapid heating of the mineral components (Haque, 1999; Lovás et al., 2011; Wang et al., 2015). It has also been found that the activation energy of a reaction is often reduced by microwave heating (Wang et al., 2018). As CFA is suitable for microwave absorption (Yakaboylu et al., 2019; Zhang et al., 2015), microwave-assisted baking is another method that can be applied to decompose CFA. It is clear that certain CFA treatment methods employing lower temperature baking lead to lower SO_3 and NH_3 emissions (van der Merwe et al., 2017; Wei et al., 2018).

This paper describes a clean strategy for reducing energy consumption and gas emissions by employing microwave-assisted baking with H_2SO_4 + NH_4HSO_4, and water leaching to extract Al and Ti from CFA. The thermodynamics of the primary reactions among reagents (H_2SO_4, NH_4HSO_4, and their mixture) indicated that H_2SO_4 and NH_4HSO_4 had synergistic effects. Experiments involving the low-temperature (<300 °C) baking of CFA with microwave heating and water leaching allowed for evaluations of the effects of the various parameters on the Al and Ti recovery. The phase changes were studied to confirm the mechanism, and the practical recovery (selective precipitation) of Al and Ti from the resulting leach liquor was investigated. The results of this study provide insights relevant for developing an efficient process to decompose CFA for metal recovery.

2. Experimental

2.1. Materials and analysis

The coal fly ash (CFA) used in this study was obtained from one of Eskom's thermal power stations in Mpumalanga, South Africa. The CFA composition was determined by X-ray Fluorescence (XRF) spectrometry, and the concentration of Al, Ti, and Fe in solid samples was determined after a total dissolution in aqua regia. Inductively coupled plasma-mass spectrometry (ICP-MS; Peculiarity Optima 5300DV, Perkin Elmer) was used to measure the concentration of the elements present in the solutions. Phase analysis of solid samples was conducted using a powder X-ray diffractometer (XRPD; PANalytical X'PERT-PRO). The mineral composition was determined by quantitative evaluation of the materials using scanning electron microscopy (SEM; QEMSCAN) analysis. The principle and procedures for QEMSCAN analysis have been reported previously by our group (Ma et al., 2018).

H_2SO_4 (96 wt%), NH_4HSO_4, iron powder, and Na_2CO_3 used in the experiments were of analytical grade. Distilled water was used in the leaching step.

2.2. Recovery procedure and thermodynamic analysis

Fig. 1 shows the proposed flowchart describing the process of recovering Al and Ti from CFA in this study. Microwave-assisted baking followed by water leaching promoted the transfer of Al and Ti to the aqueous solution in the first stage. In the baking step, a mixture of H_2SO_4 and NH_4HSO_4 was selected to digest the CFA. Next, Al^{3+} preferentially precipitated from the leach liquor via alum ($NH_4Al(SO_4)_2{\cdot}12H_2O$) precipitation after cooling at low pH. After reducing the iron in solution from Fe^{3+} to Fe^{2+} using iron powder, TiO^{2+} was selectively precipitated (over iron) by neutralization. The associated thermodynamic analyses are described in the following sections.

2.2.1. Microwave-assisted baking and leaching

It is well known that mullite is the main aluminosilicate component of CFA; however, its chemical stability poses a challenge in terms of Al extraction from CFA. The reactions describing the decomposition of mullite during the digestion of CFA with different reagents (H_2SO_4, NH_4HSO_4, and their mixture) are expressed by Eqs. (1)–(3). Ti exists in CFA mainly in the form of TiO_2, and Eq. (4) shows its reactivity during sulfation baking. The relationship between the standard Gibbs free energy change of the reactions (Δ_rG^θ) and the temperature is shown in Fig. 2. These thermodynamic data were obtained from Dean, 1985.

$$3Al_2O_3{\cdot}2SiO_2 + 9H_2SO_4 \rightarrow 3Al_2(SO_4)_3 + 2SiO_2 + 9H_2O(g) \quad (1)$$

$$3Al_2O_3{\cdot}2SiO_2 + 12NH_4HSO_4 \rightarrow 6NH_4Al(SO_4)_2 + 6NH_3(g) + 2SiO_2 + 9H_2O(g) \quad (2)$$

$$3Al_2O_3{\cdot}2SiO_2 + 6H_2SO_4 + 6NH_4HSO_4 \rightarrow 6NH_4Al(SO_4)_2 + 2SiO_2 + 9H_2O(g) \quad (3)$$

$$TiO_2 + H_2SO_4 \rightarrow TiOSO_4 + H_2O(g) \quad (4)$$

It is clear that the Δ_rG^θ values of all the reactions are negative when the temperature is less than 300 °C. For the decomposition of mullite, Eq. (2) shows that significant quantities of NH_3 are produced if NH_4HSO_4 alone is used in the reaction, which is not acceptable for practical CFA digestion. In contrast, if H_2SO_4 is used to digest CFA, no NH_3 is produced, and the molar ratio of the reagent to mullite (3:1) is lower than that (4:1) in Eq. (2). It is interesting to note that between 100 and 300 °C, the Δ_rG^θ of Eq. (3), which employs a mixture of H_2SO_4 and NH_4HSO_4, is lower than those of Eq. (1) and (2), and the reaction product is $NH_4Al(SO_4)_2$, thus avoiding emission of NH_3. Another issue in the reactions involving H_2SO_4 is that the decomposition of H_2SO_4 at high temperature produces SO_3 (boiling point of H_2SO_4 = 338 °C). Therefore, baking below 300 °C with a mixture of NH_4HSO_4 and H_2SO_4 was the best strategy for decomposing mullite.

A laboratory microwave oven (NAI-SYS-WBL microvave oven, Naai Instrument Co. Ltd., Shanghai, China) with a frequency of 2.45 GHz was used for low-temperature baking of the reaction mixtures. The heating rate and temperature could be controlled by adjusting the microwave oven's output power; alternatively, it was possible to bake the mixture using a constant output power. A schematic drawing of the experimental apparatus is shown in Fig. 3. The temperatures of the reactants and the microwave chamber were monitored using thermocouples (Thermocouples 1 and 2 in Fig. 3). The mass of the CFA used in each experiment was 50 g. After adding all the reagents, the mixture was heated using microwaves with a constant output power of 100 W. Considering the exothermic reactions during CFA digestion, the output power was reduced to 0 W when the temperature of the mixture reached

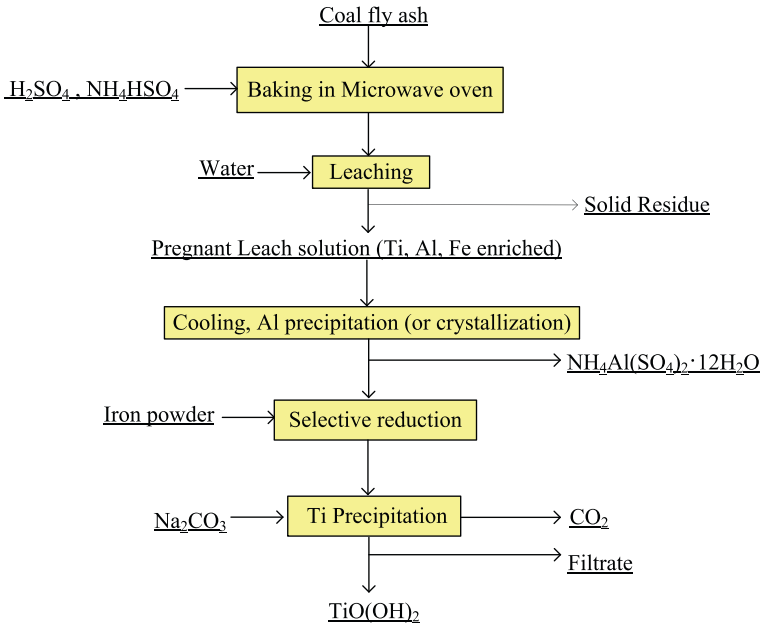

Fig. 1. Proposed flowchart for recovering Al and Ti from CFA.

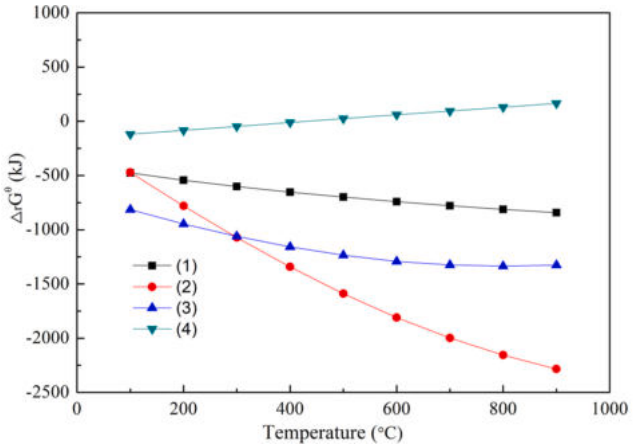

Fig. 2. Relationship between the standard Gibbs free energy of the reactions ($\Delta_r G^\theta$) and the temperature.

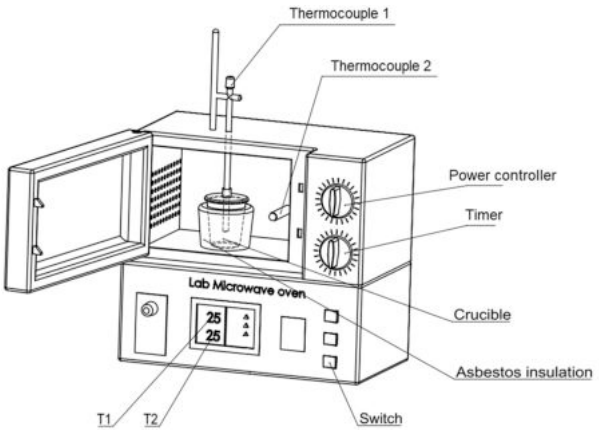

Fig. 3. Schematic drawing of the baking apparatus.

~20 °C below the specified baking temperature. After the specified temperature was reached, the mixture was then maintained automatically for a designated amount of time by intermittent heating (100 W output).

It was expected that $Al_2(SO_4)_3$, $NH_4Al(SO_4)_2$, and $TiOSO_4$ would form after sulfation baking. The baked CFA was subsequently dissolved in distilled water, which allowed for the leaching of Al and Ti. A leachate was obtained after vacuum filtering and washing the filter cake. The filtrate was collected and analyzed to determine the extraction efficiency. The extraction efficiency was calculated by element quality in leachate versus element quality in the CFA used:

$$\text{Extraction efficiency} = \frac{\text{C(considered metal in solution)} \bullet \text{V(filtrate)}}{\text{m(CFA)} \bullet \omega\text{(considered metal in CFA)}}$$

where C = concentration, V = volume, m = mass and ω = mass fraction.

2.2.2. Selective precipitation of Al and Ti

The resulting leach solution contained Al^{3+}, TiO^{2+}, and some impurities, such as Na^+, Ca^{2+}, and Fe^{3+}. The Al^{3+} could be recovered from the leach liquor via $NH_4Al(SO_4)_2$ alum precipitation after cooling at low pH, because the water solubility of $NH_4Al(SO_4)_2 \cdot 12H_2O$ is highly dependent on the temperature. As shown in Table 1, the solubility of $NH_4Al(SO_4)_2 \cdot 12H_2O$ is only 2.4 g per 100 g water at 0 °C. As a result, most of the Al can precipitate as crystals at 0 °C, thereby avoiding co-precipitation with other metal ions. This method is favored over Al $(OH)_3$ precipitation because it proceeds without neutralization, and the crystalline $NH_4Al(SO_4)_2 \cdot 12H_2O$ is easier to filter than the gelatinous Al $(OH)_3$. In this study, the CFA leach solution was maintained at 0 °C for 10 h to obtain alum crystals.

Metal hydroxide precipitation is a common method for preliminary separation and enrichment of metal from aqueous solution in hydro-

Table 1
Solubility of $NH_4Al(SO_4)_2 \cdot 12H_2O$ (Poling et al., 2008).

Temperature (°C)	0	20	40	60	80	100
Solubility (g/100 g H_2O)	2.4	7.4	14.6	26.7	53.9	121

metallurgy. The log[M^{n+}]-pH diagram based on the solubility product constants of metal hydroxides at 298.15 K is shown in Fig. 4. The pH ranges for Ti^{3+}, TiO^{2+}, and Fe^{3+} hydrolysis are quite close, so direct neutralization cannot achieve Ti precipitation over Fe^{3+} precipitation. However, the pH range for Fe^{2+} hydrolysis is much higher than that for TiO^{2+} and Ti^{3+}, so reducing the iron from Fe^{3+} to Fe^{2+} prior to neutralization could prevent co-precipitation. Fig. 5 presents the potential-pH diagram of the Ti-H_2O system at 298.15 K and low pH (the electrode potentials of $E^0(Fe^{3+}/Fe^{2+}) = 0.77$ V, $E^0(Fe^{2+}/Fe) = -0.46$ V) (Dean, 1985). Based on this diagram, TiO^{2+} and Fe^{2+} can co-exist if the pH and potential are controlled in the red hashed area in Fig. 5, but Ti^{3+} and Fe^{3+} cannot co-exist at low pH because there is no overlap in their respective predominant areas in the diagram. The addition of iron powder to the solution would reduce Fe^{3+} to Fe^{2+}, and TiO^{2+} is colorless, but Ti^{3+} is purple in an aqueous solution. Therefore, a slight excess of iron powder was added to react with the solution until the solution appeared purple, indicating that all iron was reduced to Fe^{2+}, and a little Ti^{3+} was produced. The small amount of Ti^{3+} produced could be transformed back into TiO^{2+} after adding the initial solution slowly until the purple color disappeared. In this way, the Ti-bearing solution was controlled in the red hashed area of Fig. 5. Next, TiO^{2+} was precipitated (over Fe^{2+}) from the solution by adjusting the pH to around 3.0. The relevant reactions are represented by Eq. (5) and Eq. (6).

$$Fe + Fe^{3+} \rightarrow 2Fe^{2+} \quad (5)$$

$$TiO^{2+} + 2OH^- \rightarrow TiO(OH)_{2\,(s)} \quad (6)$$

3. Results and discussion

3.1. Characterization of coal fly ash

The chemical composition of the CFA used in this work is listed in Table 2, which revealed 32.1 wt% Al_2O_3 and 1.68 wt% TiO_2. Fig. 6 shows the phase distribution determined based on QEMSCAN analysis, and the proportion of phases are summarized in Table 3. The major phases in the CFA were mullite, quartz, and other aluminosilicate phases. Two SEM images of the CFA are shown in Fig. 7. The CFA, which consisted of various spheres with smooth surfaces, embodied the typical microstructure of a vitreous body. Fig. 6 also shows that mullite and rutile were embedded heterogeneously within these spheres.

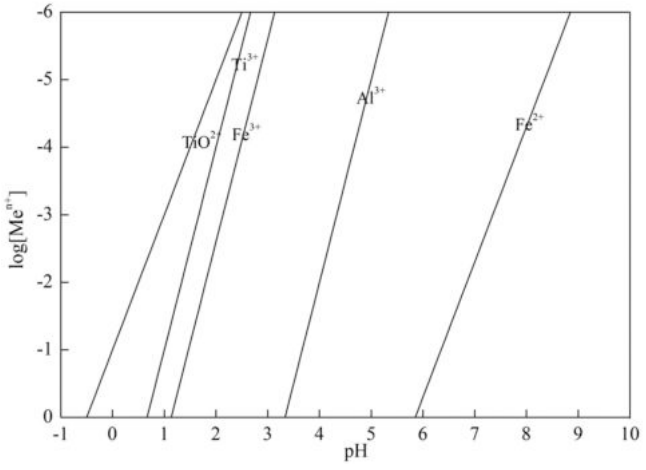

Fig. 4. log[Me^{n+}]-pH diagram based on the solubility product constants (K_{sp}) of metal hydroxides at 298.15 K (K_{sp} values obtained from Dean, 1985).

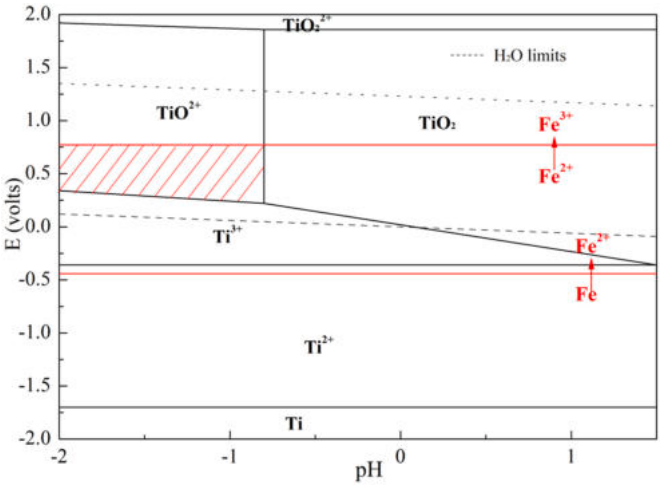

Fig. 5. *E*-pH diagram of the Ti-H_2O and Fe-H_2O systems at 298.15 K and low pH (Activities: titanium 0.001, iron 0.01).

Table 2
Chemical composition of the raw CFA and the residue after leaching in this study[a].

Sample	Oxide composition (% *w*/w)						
	Al_2O_3	SiO_2	CaO	Fe_2O_3	MgO	TiO_2	L.O.I.[b]
Raw CFA	32.1	55.2	3.44	6.04	1.07	1.68	1.40
Leach residue	7.15	71.87	4.34	2.89	1.33	0.91	8.40

[a] On dry base.
[b] Loss on ignition.

3.2. Sulfation baking via microwave heating and leaching

3.2.1. Comparative results

To confirm the advantages of the proposed strategy, some preliminary tests were performed to compare the heating rates of the materials and the performances of different reagents. Fig. 8 shows the comparative heating curves (mass of CFA used in the heating experiments = 50 g). It is clear that microwave radiation was sufficient to rapidly heat the CFA (or the mixture of CFA and reagents), while the temperature of the microwave chamber (T_2) was kept very low. Therefore, selective microwave heating contributed to efficient energy use during the baking process. On the other hand, the temperature of the reactants increased continuously even though the microwave oven's output was reduced to 0 W output once it reached 260 °C (Fig. 8). This was because of the heat generated by the exothermic reactions occurring during CFA digestion; the microwave-assisted baking technique took full advantage of the exothermic effect of the reactions, which is not possible in conventional heating.

The comparative results from microwave heating versus conventional heating, and the performance of different reagents are summarized in Fig. 9. The conventional heating experiment was conducted in a muffle furnace (Nabertherm™ L-051H1RN1T, Nabertherm LLC., Lilienthal, Germany), and all other experimental parameters were unchanged. The amount of each reagent added to the mixture was 1.2 times the theoretical values calculated considering the Al_2O_3 and TiO_2 content in the CFA and the stoichiometry of Eqs. (1)–(4). The theoretical values of these three kinds of extraction reagents per 100 g CFA are 98.5 g H_2SO_4 (96 wt%) per 100 g CFA, 144.8 g NH_4HSO_4 per 100 g CFA, and 66.4 g H_2SO_4 (96 wt%) + 72.4 g NH_4HSO_4, respectively. The baking temperature and time were 280 °C and 60 min, respectively. Water leaching proceeded for 30 min at 60 °C with a liquid to solid ratio of 5 g water to 1 g baked ash. It is clear from Fig. 9 that the application of microwave heating enhanced the CFA digestion in terms of Al and Ti

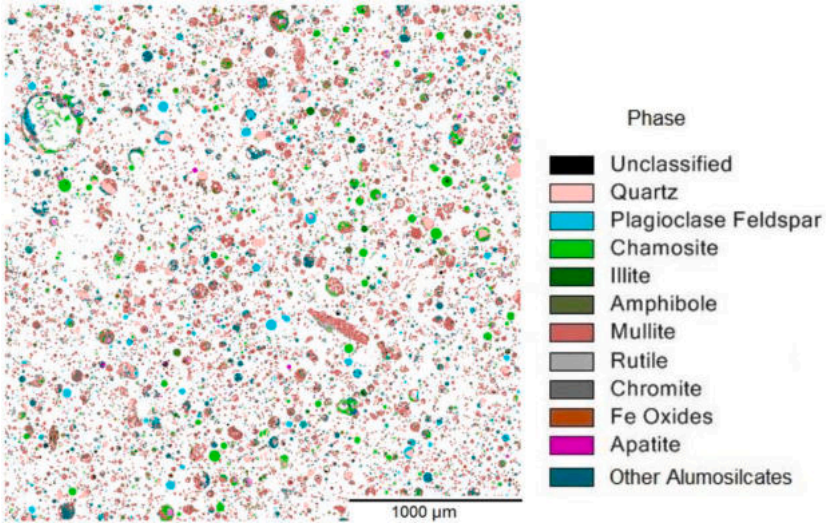

Fig. 6. QEMSCAN analysis of the CFA by false color imaging.

Table 3
Phase distribution of the CFA.

Mineral	Proportion (%)
Unclassified	3.53
Quartz	13.3
Plagioclase Feldspar	4.59
Chamosite	7.71
Illite	1.67
Amphibole	1.52
Mullite	51.6
Rutile	0.78
Fe Oxides	1.29
Apatite	0.51
Other Alumosilcate	13

extraction compared with conventional heating. The extraction efficiency was the highest when the mixture of H_2SO_4 and NH_4HSO_4 was used as the extractant; the extraction efficiency was much lower after baking with only NH_4HSO_4. These results indicated that the solid-solid reaction performance was inferior to the solid-liquid reaction. Overall, the comparative results were consistent with the thermodynamic analysis presented in Fig. 2, and it was concluded that baking with the mixture of NH_4HSO_4 and H_2SO_4 was the optimal choice for CFA digestion.

3.2.2. *Effect of baking temperature on Al and Ti extraction*

The effect of the baking temperature on Al and Ti extraction was tested using 1.2 times the theoretical amount of H_2SO_4 + NH_4HSO_4 calculated from Eqs. (1)–(4). The baking time was set constant at 60 min. As shown in Fig. 10, the Al extraction efficiency increased from 67.4% to 82.4% as the temperature increased from 220 to 280 °C, but no additional enhancement was observed upon increasing the temperature further to 300 °C. The Ti extraction efficiency increased from 43.1% to 55.6% as the temperature increased from 220 to 280 °C; however, upon further increasing to 300 °C, the Ti extraction efficiency decreased slightly. These results were consistent with a published report that Ti extraction efficiency was lower at a higher temperature (van der Merwe et al., 2017). Finally, the optimal baking temperature was determined to be 280 °C.

3.2.3. *Effect of reagent quantities on Al and Ti extraction*

During the baking process, all phases except mullite and rutile in the CFA could consume reagents; therefore, it was necessary to add more than the stoichiometrically-required amounts of reagents (H_2SO_4 + NH_4HSO_4) calculated based on the Al_2O_3 and TiO_2 content in the CFA. The effect of reagent quantities on Al and Ti extraction is illustrated in Fig. 11, which indicates that aluminum extraction increased upon increasing the excess ratio of reagents. For example, the Al extraction efficiency was 73.8% using the theoretically-determined reagent quantities, and increased to 82.4% when the excess ratio increased to 1.2 (no further increase in efficiency was observed with a further increase in the excess ratio to 1.4). The results also showed that the amounts of reagents had little effect on the Ti extraction efficiency; the addition of excess reagents was not necessary. Therefore, the optimal excess ratio was 1.2,

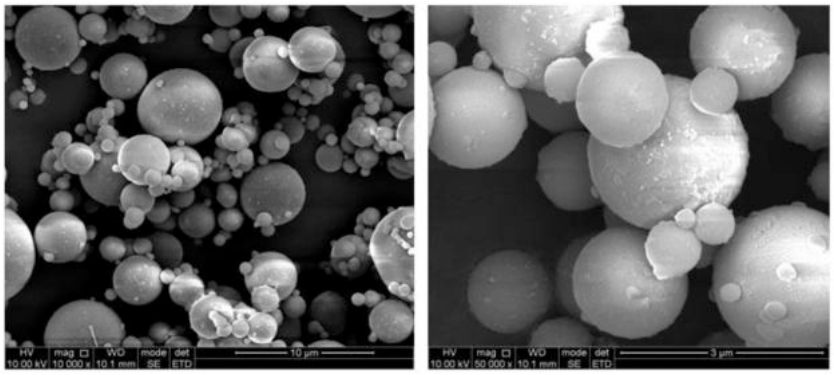

Fig. 7. SEM images of the CFA.

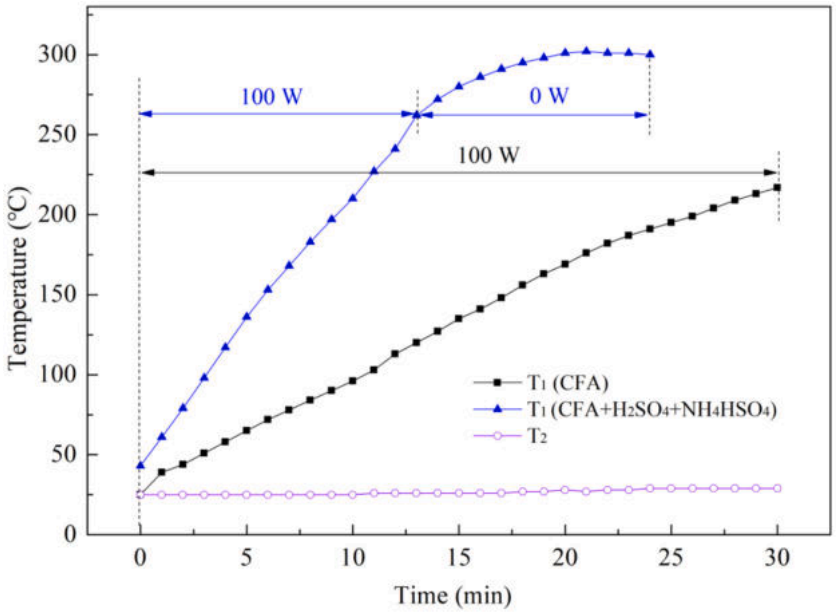

Fig. 8. Heating curves for CFA and the mixture of CFA with reagents (T_1: the temperature of the reactants, T2: the temperature of the microwave chamber).

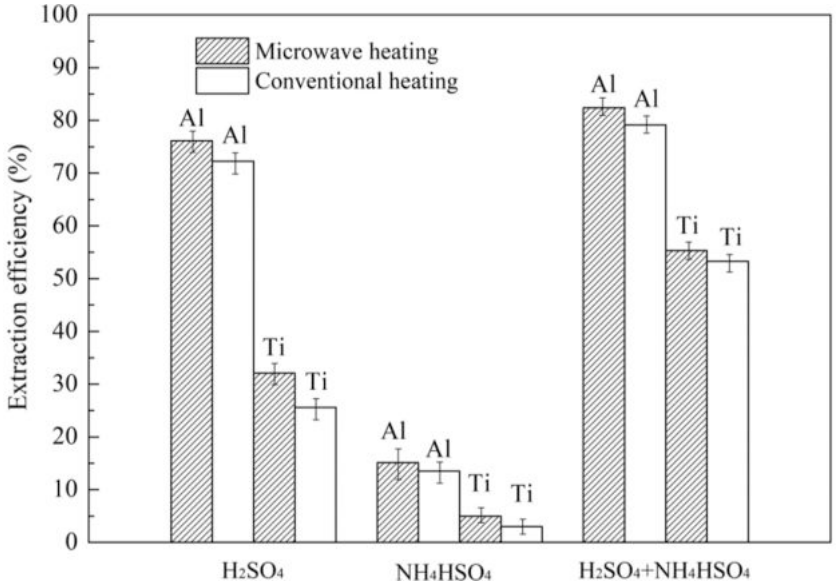

Fig. 9. Comparative results, baking conditions: 280 °C, 1.2 times the theoretical amount of reagents, 60 min, leaching conditions: 60 °C, L/S: 5 g water to 1 g baked ash, 30 min.

which enabled maximal Al and Ti extraction while saving reagents.

3.2.4. *Effect of baking time on Al and Ti extraction*

The effect of the baking time on Al and Ti extraction from the CFA was evaluated experimentally, and the results are shown in Fig. 12. When using H_2SO_4 + NH_4HSO_4 to digest the CFA, both the Al and Ti extraction efficiencies increased with prolonged baking time. The digestion performance did not increase further with baking times longer than 60 min, so this baking time was the most logical for Al and Ti extraction using microwave heating.

3.2.5. *Effect of leaching conditions on Al and Ti extraction*

It has been demonstrated that leaching conditions are typically not critical variables for the extraction of metals from CFA after acid digestion (Wei et al., 2018). In this investigation, 60 °C was the optimal temperature for the leaching process, which was nearly completed in 30 min. Liquid-solid ratios ranging from 1 to 10 g of water to 1 g baked ash were tested. There was no significant change in Al or Ti extraction when the water used was over 5 times the amount of baked ash. The high concentration of Al in the leach solution promoted the subsequent crystallization of $NH_4Al(SO_4)_2{\cdot}12H_2O$. The optimal liquid-solid ratio was ultimately set to 5 g water to 1 g baked ash. Under these leaching conditions, and after filtering and washing the filter cake, the Al and Ti extraction efficiencies reached 83.4% and 55.6%, respectively. The leach residue contained a large proportion of silica (71.9%), but the content of alumina decreased to 7.2% (Table 2). It could be used as a secondary source of e.g. nano-silica, or as an additive in the cement industry.

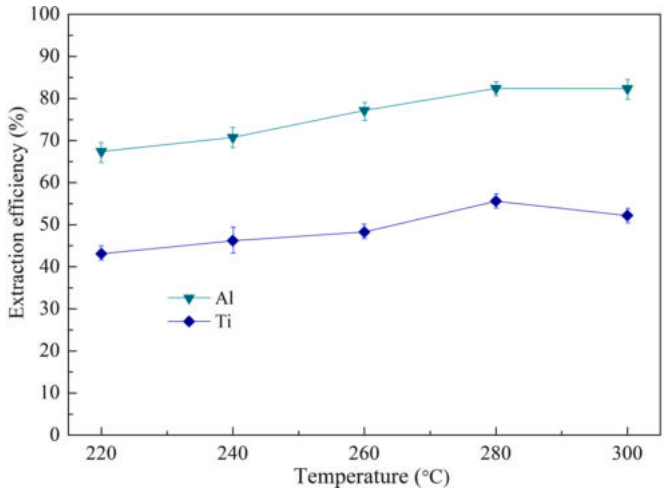

Fig. 10. Effect of baking temperature on Al and Ti extraction efficiencies, baking conditions: 1.2 times the theoretical amount of reagents, 60 min, leaching conditions: 60 °C, L/S: 5 g water to 1 g baked ash, 30 min.

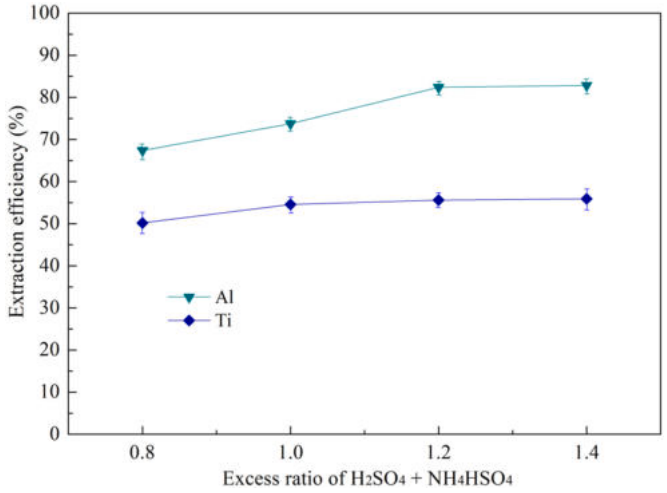

Fig. 11. Effect of reagent quantities on Al and Ti extraction efficiencies, baking conditions: 280 °C, 60 min, leaching conditions: 60 °C, L/S: 5 g water to 1 g baked ash, 30 min.

3.3. Morphological evidence and phase changes

The microstructures of the baked CFA and the residue after leaching were characterized by SEM (Fig. 13) to observe changes in their morphologies. After microwave-assisted sulfation baking, many of the spherical particles in the CFA were replaced by significant amounts of polygonal and square pellets, and some spheres shrank in size. This change in morphology indicated mullite decomposition and the formation of new sulfate salts. Fig. 14 shows the XRD patterns of the raw CFA, baked CFA, and leach residue. The major phase components of the raw CFA were quartz, mullite, hematite, and amorphous glass. This result was in good agreement with the QEMSCAN results, although the small amount of rutile was hard to identify by XRD analysis. After baking, the newly formed pellets existed mainly as crystalline godovikovite ($NH_4Al(SO_4)_2$), millosevichite ($Al_2(SO_4)_3$), anhydrite ($CaSO_4$), and quartz (SiO_2). The peak intensity of the remaining mullite in the baked CFA was much lower than that of other phases. It was also inferred that there was a small amount of $TiOSO_4$ in the baked CFA. These newly formed phases interlocked around the spheres to form clusters visible in the SEM images, and some covered some of the initial spheres, which may have

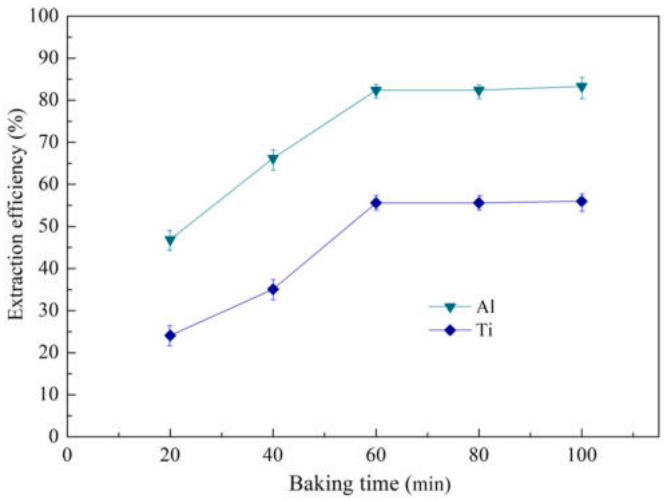

Fig. 12. Effect of baking time on Al and Ti extraction, baking conditions: 280 °C, 1.2 times the theoretical amount of reagents, leaching conditions: 60 °C, L/S: 5 g water to 1 g baked ash, 30 min.

hampered acid diffusion, thus explaining the incomplete extraction of Al and Ti.

After leaching, the soluble godovikovite was dissolved into the solution, and the corresponding peaks in the XRD pattern disappeared. The leach residue's XRD pattern (Fig. 14) indicated that a small amount of mullite and hematite remained in the residue. The sizes of the remaining spheres were smaller than those in raw CFA, which confirmed the sphere shrinkage; some spheres also collapsed. The scratches marked with red circles on the surface of the CFA particles represent clear indications of mullite removal. These SEM images were consistent with previous work applying acid baking and leaching (Bai et al., 2011).

3.4. Selective precipitation of Al and Ti from the leach solution

After leaching, precipitation methods were used to recover and isolate Al and Ti from the leach solution. The chemical composition of the experimental solutions is listed in Table 4. Al was precipitated selectively (92.2%) at 0 °C after 10 h. The phase of the alum crystals was determined by XRD analysis (Fig. 15); these crystals were calcined at 800 °C for 3 h and analyzed further using XRF. The composition of the calcined alumina is presented in Table 5, and the Al_2O_3 content was 99.6%, which meets the requirements of industrial alumina. After reducing the Fe^{3+}, the pH was adjusted to 3.11 by adding Na_2CO_3 to precipitate Ti^{4+} in a 97.9% yield. Table 6 shows the composition of the resulting precipitate; the content of Ti was 44.2%, and the content of other impurities was low, but further purification was necessary to obtain the desired Ti product. In this way, the gelatinous $Fe(OH)_3$ was prevented from getting into the Ti-rich precipitate, which was beneficial to the subsequent Ti recovery and purification.

4. Conclusions

In this paper, we described a clean and energy-efficient process for recovering Al and Ti from CFA. Microwave heating and using a mixture of H_2SO_4 + NH_4HSO_4 as the extraction agent reduced the energy consumption and gas emissions associated with the conventional process, and this method also enhanced the Al and Ti extraction efficiencies compared with other acidic baking strategies. The optimal microwave-assisted baking conditions were: 280 °C, 1.2 times the theoretical amount of reagents, 60 min. The primary phase formed after microwave-assisted baking was godovikovite ($NH_4Al(SO_4)_2$). After water leaching, 82.4% Al and 55.6% Ti could be extracted when applying the optimal baking and leaching parameters.

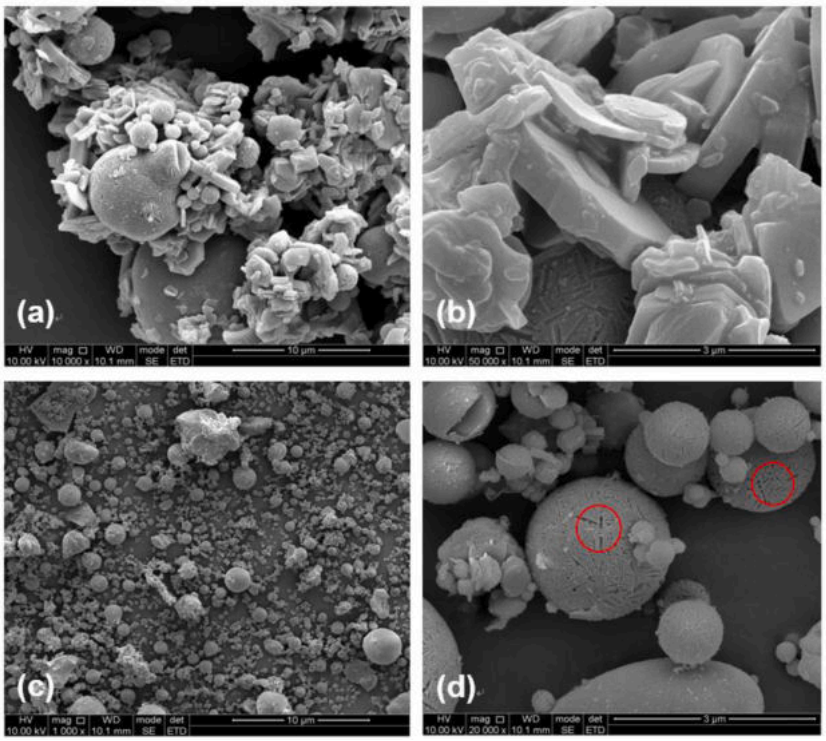

Fig. 13. SEM images of solid samples: (a,b) baked CFA; (c,d) residue after water leaching. Note: the scratches on the surface of the CFA particles are marked with red circles. (For interpretation of the references to color in this figure legend, the reader is referred to the web version of this article.)

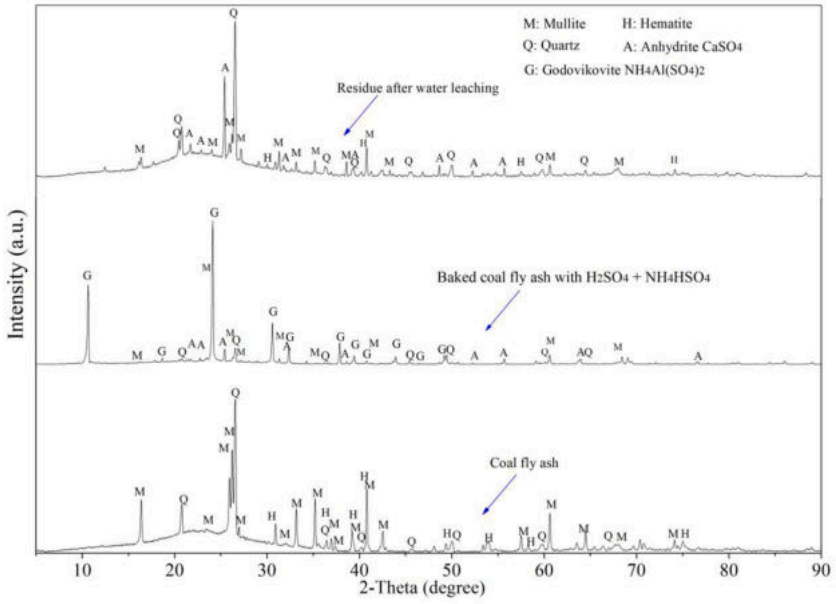

Fig. 14. XRD patterns of the raw CFA (bottom), microwave-assisted baked CFA (middle), and leach residue (top).

Table 4
Chemical composition of experimental solutions.

Element	Elemental analysis (g/L)							
	Al	Fe(II)	Fe(III)	Ti	Ca	Mg	S	pH
CFA leach solution	10.7	0.12	2.51	0.44	<0.005	<0.005	38.5	0.64
After precipitation of Al	0.84	0.13	2.72	0.48	<0.005	<0.005	15.1	0.63
After reduction of Fe(III)	0.84	4.22	<0.001	0.48	<0.005	<0.005	15.1	0.74
After precipitation of Ti	0.80	4.10	<0.001	0.01	<0.005	<0.005	15.1	3.11

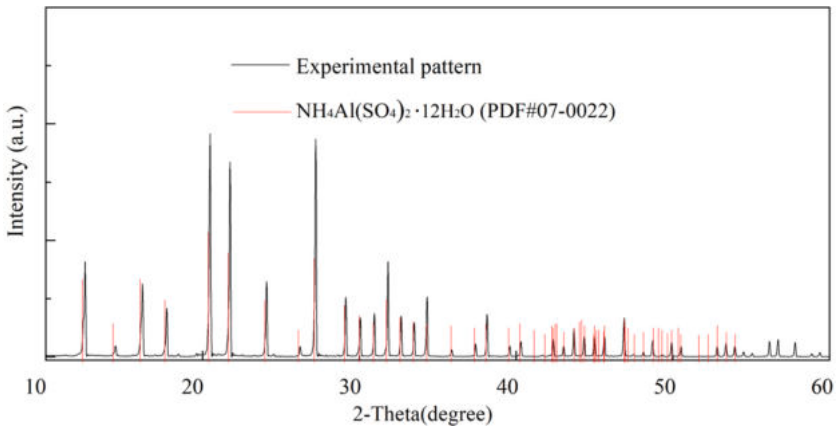

Fig. 15. XRD pattern of the alum crystals.

Table 5
Chemical composition of calcined alumina.

Composition	Al_2O_3	Na_2O	Fe_2O_3	CaO	TiO_2	SiO_2	MgO	P_2O_5	SO_3
Content (wt%)	99.6	0.25	0.02	0.01	0.01	0.02	0.01	0.001	0.05

Table 6
Chemical composition of the Ti precipitate.

Element	Ti	Fe	Al	Si	Ca	Mg	Na
Content (wt%)	44.2	0.11	0.05	<0.005	0.12	0.01	3.12

Taking advantage of the NH_4^+ in the resulting leach solution, Al was selectively recovered via $NH_4Al(SO_4)_2{\cdot}12H_2O$ precipitation after maintaining the solution at 0 °C for some time. A high-quality alumina product could then be obtained from the $NH_4Al(SO_4)_2{\cdot}12H_2O$. After reducing the iron in the solution from Fe^{3+} to Fe^{2+}, Ti was recovered via hydrolysis after increasing the pH. The Ti precipitate contained 44.2% Ti, which required further treatment to obtain the final pure product.

In conclusion, the developed technology was highly beneficial in terms of enhancing the efficient recovery of Al and Ti from CFA, while also reducing the processing costs and harmful gas emissions.

Author statement

None.

Declaration of Competing Interest

None.

Acknowledgments

The authors are thankful to Eskom, South Africa, for providing the initial material. This research was funded by the International Office of the BMBF in Germany, grant number: 01DG17024, and by NRF in South Africa, grant number GERM160705176077.

References

Bai, G., Qiao, Y., Shen, B., Chen, S., 2011. Thermal decomposition of coal fly ash by concentrated sulfuric acid and alumina extraction process based on it. Fuel Process. Technol. 92, 1213–1219.
Cavusoglu, I., Yilmaz, E., Yilmaz, A.O.J.C., Materials, B., 2020. Additivity effect on properties of cemented coal fly ash backfill containing water-reducing admixtures. Constr. Build. Mater. 267, 121021.
Dean, J., 1985. Langes's Handbook of Chemistry, 13th ed. McGraw-Hill, Inc., New York, NY, USA.
Ding, J., Ma, S., Shen, S., Xie, Z., Zheng, S., Zhang, Y., 2017. Research and industrialization progress of recovering alumina from fly ash: a concise review. Waste Manag. 60, 375–387.
Doucet, F.J., Mohamed, S., Neyt, N., Castleman, B.A., Merwe, E.M., 2016. Thermochemical processing of a south African ultrafine coal fly ash using ammonium sulphate as extracting agent for aluminium extraction. Hydrometallurgy 166, 174–184.
Eskom, 2017. Exploring the many uses of fly ash. Ee publishers (obtained from www.eskom.co.za, on 22.11.2017).
European Commission, 2020. Critical raw materials. https://ec.europa.eu/growth/sectors/raw-materials/specific-interest/critical_en.
Guo, Y., Zhao, Z., Zhao, Q., Cheng, F., 2017. Novel process of alumina extraction from coal fly ash by pre-desilicating—Na2CO3 activation—acid leaching technique. Hydrometallurgy 169, 418–425.
Gupta, V., Pathak, D.K., Siddique, S., Kumar, R., Chaudhary, S.J.C., Materials, B., 2020. Study on the mineral phase characteristics of various Indian biomass and coal fly ash for its use in masonry construction products. Constr. Build. Mater. 235, 117413.
Haque, K.E., 1999. Microwave energy for mineral treatment processes—a brief review. Int. J. Miner. Process. 57, 1–24.
Lekgoba, T., Ntuli, F., Falayi, T., 2020. Application of coal fly ash for treatment of wastewater containing a binary mixture of copper and nickel. J. Water Process. Eng. 101822.
Li, H., Hui, J., Wang, C., Bao, W., Sun, Z.J.H., 2014. Extraction of alumina from coal fly ash by mixed-alkaline hydrothermal method. Hydrometallurgy 147, 183–187.
Lovás, M., Znamenáčková, I., Zubrik, A., Kováčová, M., Dolinská, S., 2011. The application of microwave energy in mineral processing – a review. Acta Montan. Slovaca 16, 137–148.
Ma, Y., Stopic, S., Gronen, L., Friedrich, B., 2018. Recovery of Zr, Hf, Nb from eudialyte residue by sulfuric acid dry digestion and water leaching with H_2O_2 as a promoter. Hydrometallurgy 181, 206–214.
Matjie, R.H., Bunt, J.R., Heerden, J.H.P., 2005. Extraction of alumina from coal fly ash generated from a selected low rank bituminous south African coal. Miner. Eng. 18, 299–310.
Mishra, R.R., Sharma, A.K., 2016. Microwave–material interaction phenomena: heating mechanisms, challenges and opportunities in material processing. Compos. Part A Appl. Sci. Manuf. 81, 78–97.
Padilla, R., Sohn, H.Y., 1985. Sintering kinetics and alumina yield in lime-soda sinter process for alumina from coal wastes. Metall. Trans. B 16, 385–395.
Poling, B.E., Thomson, G.H., Friend, D.G., 2008. Perry's Chemical Engineers' Handbook, Physical and Chemical Data, 8th ed. McGraw-Hill, New York.
Rahaman, M.A., Gafur, M.A., Kurny, A.S.W., 2013. Kinetics of recovery of alumina from coal Fly ash through fusion with sodium hydroxide. Am. J. Mater. Sci. 3, 54–58.
Rampou, M., Ndlovu, S., Shemi, A., 2017. Purification of coal Fly ash leach liquor for alumina recovery using an integrated precipitation and solvent extraction process. J. Sustain. Metall. 3, 782–792.
Sahoo, P.K., Kim, K., Powell, M.A., Equeenuddin, S.M., 2016. Recovery of metals and other beneficial products from coal fly ash: a sustainable approach for fly ash management. Int. J. Coal Sci. Technol. 3, 267–283.
Shemi, A., Mpana, R.N., Ndlovu, S., Dyk, L.D., Sibanda, V., Seepe, L., 2012. Alternative techniques for extracting alumina from coal fly ash. Miner. Eng. 34, 30–37.
Shemi, A., Ndlovu, S., Sibanda, V., Dyk, L.D., 2015. Extraction of alumina from coal fly ash using an acid leach-sinter-acid leach technique. Hydrometallurgy 157, 348–355.

Shi, Y., Jiang, K.-X., Zhang, T.-A., Lv, G.-Z., 2020. Cleaner alumina production from coal fly ash: membrane electrolysis designed for sulfuric acid leachate. J. Clean. Prod. 243, 118470.
Taggart, R.K., Hower, J.C., Hsu-Kim, H., 2018. Effects of roasting additives and leaching parameters on the extraction of rare earth elements from coal fly ash. Int. J. Coal Geol. 196, 106–114.
van der Merwe, E.M., Gray, C.L., Castleman, B.A., Mohamed, S., Kruger, R.A., Doucet, F. J., 2017. Ammonium sulphate and/or ammonium bisulphate as extracting agents for the recovery of aluminium from ultrafine coal fly ash. Hydrometallurgy 171, 185–190.
Wang, M., Xian, P., Wang, X., Li, B., 2015. Extraction of vanadium from stone coal by microwave assisted Sulfation roasting. JOM 67, 369–374.
Wang, J., Zhang, Y., Liu, T., Huang, J., 2018. Evaluation of microwave intensified vanadium bearing-high carbonaceous shale acid extraction process. Minerals 8, 113.
Wei, C., Cheng, S., Zhu, F., Tan, X., Li, W., Zhang, P., Miao, S., 2018. Digesting high-aluminum coal fly ash with concentrated sulfuric acid at high temperatures. Hydrometallurgy 180, 41–48.
Xue, Y., Yu, W., Mei, J., Jiang, W., Lv, X.J., Jo, C.P., 2019. A clean process for alumina extraction and ferrosilicon alloy preparation from coal fly ash via vacuum thermal reduction. J. Clean. Prod. 240, 118262.
Yadav, V.K., Fulekar, M.H., 2020. Advances in methods for recovery of ferrous, alumina, and silica nanoparticles from Fly ash waste. Ceramics 3, 384–420.
Yakaboylu, G.A., Baker, D., Wayda, B., Sabolsky, K., Zondlo, J.W., Shekhawat, D., Wildfire, C., Sabolsky, E.M., 2019. Microwave-assisted pretreatment of coal Fly ash for enrichment and enhanced extraction of rare-earth elements. Energy Fuel 33, 12083–12095.
Yao, Z., Xia, M., Sarker, P., Chen, T., 2014. A review of the alumina recovery from coal fly ash, with a focus in China. Fuel 120, 74–85.
Yao, Z.T., Ji, X.S., Sarker, P.K., Tang, J.H., Ge, L.Q., Xia, M.S., Xi, Y.Q., 2015. A comprehensive review on the applications of coal fly ash. Earth Sci. Rev. 141, 105–121.
Zhang, Z., Qiao, X., Yu, J., 2015. Aluminum release from microwave-assisted reaction of coal fly ash with calcium carbonate. Fuel Process. Technol. 134, 303–309.
Zhou, Y., Yang, H., Xue, X.-X., Yuan, S., 2017. Separation and recovery of Iron and rare earth from Bayan obo tailings by magnetizing roasting and $(NH_4)_2SO_4$ activation roasting. Metals 7, 195.